Correlation between the nanoscale structure and the optical properties of Ce-doped $SiO_{1.5}$ thin films

Georges Beainy [a], Jennifer Weimmerskirch-Aubatin [b], Mathieu Stoffel [b], Michel Vergnat [b], Hervé Rinnert [b], Philippe Pareige [a], Etienne Talbot [a,*]

[a] Normandie Univ, UNIROUEN, INSA Rouen, CNRS, Groupe de Physique des Matériaux, 76000 Rouen, France
[b] Université de Lorraine, UMR CNRS 7198, Institut Jean Lamour, BP 70239, 54506 Vandœuvre-lès-Nancy, France

A B S T R A C T

Cerium doped SiO_x ($0 < x < 2$) thin films have emerged as promising materials for future Si-based blue light emitting devices. The optical properties of these films are strongly dependent on the nanoscale structure such as the spatial distribution of the Ce atoms. These issues have remained difficult to observe in practice by conventional techniques. In this work, we propose to use atom probe tomography which has emerged as a unique technique that is able to provide information about the chemical composition of the films together with a 3D map indicating the position of each atom from a specimen. Ce-doped $SiO_{1.5}$ thin films fabricated by evaporation were investigated. The effect of Ce-content has been systematically studied in order to correlate the structure at the nanoscale with the optical properties measured by photoluminescence spectroscopy.

1. Introduction

As a material of choice in modern microelectronics, silicon (Si) has attracted increasing attention during the last decades. The interest was mainly driven by the possibility to integrate both optoelectronic and microelectronic functionalities on a same Si chip. Due to its indirect bandgap, bulk Si is a poor light emitter. The development of an efficient Si-based light emitter is therefore a challenging issue. Following Canham's discovery in 1990 of light emission in porous silicon [1], there has been a substantial interest on nanostructured silicon as promising material to circumvent the limitations of bulk Si. Pure Si nanocrystals (Si-ncs) embedded in a SiO_2 matrix are shown to have an appreciable and steady light emission at room temperature [2–5] and are moreover compatible with the Si technology. Although an optical gain was claimed with Si-ncs [6], there is still no efficient light emitting device available based on Si-ncs. Furthermore, the emission of Si-ncs is limited to a narrow spectral range between 600 and 850 nm.

Doping with optically active ions such as rare earth ions is a promising alternative approach to obtain an efficient optical emission from Si-based materials due to their outstanding optical properties. Rare earth (RE) doped Si-based insulating matrices such as silicon oxide (SiO_2), silicon-rich silicon oxide (SiO_x), silicon nitride (Si_3N_4) and silicon-rich silicon nitride (SiN_x) have been extensively investigated. In such matrices, RE photoluminescence emission has been evidenced in the ultraviolet, visible and near-infrared spectral ranges [7–10]. Moreover, efficient electroluminescence in the UV (~320 nm), blue (~440 nm), green (~550 nm), red (~620 nm) and IR (~1540 nm) range has been demonstrated in metal-oxide-semiconductor (MOS) devices with SiO_2 implanted with rare earth elements such as Gd [9], Ce+Gd [10], Tb [11], Eu [12] and Er [13]. Although, the three primary colors (red, green and blue) can be achieved by the same device structure, expensive ion-implantation equipment for the high dose implantation of rare earth elements is required in MOS devices with rare earth ion implanted SiO_2.

Moreover, it has been reported that rare earth silicates can present higher optically active rare ions than that observed in rare earth doped matrices [14–17]. This can be a new promising approach and an effective way for rare earth applications in photonic devices.

Among all rare earth atoms, cerium (Ce) is of particular interest since Ce^{3+} ions are characterized by an allowed electric dipolar 5d–4f transition giving rise to emission in the violet-blue range. Morshed et al. reported photoluminescence (PL) near 400 nm by depositing CeO_2 layer on a Si (111) substrate by pulsed laser deposition and annealing in argon ambient at 1000 °C [18]. The

* Corresponding author.
E-mail address: etienne.talbot@univ-rouen.fr (E. Talbot).

http://dx.doi.org/10.1016/j.jlumin.2016.10.017

luminescence was attributed to the formation of a Ce_6O_{11} phase. Later, Choi et al. reported violet-blue luminescence in Ce oxide films fabricated by radio-frequency sputtering [19]. The luminescence was attributed to the formation of Ce-silicates. Similar observations were made in other studies [17,20,21].

Recently, we have investigated the effect of post growth annealing treatment on the nanostructure and the optical properties of 3 at.% Ce-doped $SiO_{1.5}$ thin films [22–24]. We have demonstrated the formation of Ce-disilicate nanoparticles through a complex phase separation between the Si in excess, Ce atoms and the SiO_2 matrix. Moreover, following a quenching of the Ce-related luminescence with annealing temperatures up to 980 °C, an intense emission was found to reappear after annealing at 1100 °C. By examining the nanostructure of the films with Atom Probe Tomography (APT), we have attributed the intense luminescence to the formation of a Ce-disilicate phase of stoichiometry $Ce_2Si_2O_7$.

To go further insight in the growth and luminescence of cerium silicates nanoparticles in Ce-doped SiO_x films, we perform in this work an atomic scale investigation of Ce-doped $SiO_{1.5}$ thin films as a function of Ce content by means of APT for a constant silicon excess of ~10%. The obtained nanostructure by APT was then correlated with the optical properties of the analyzed samples. Our overall objective is to focus on the evolution of the nanostructure in such systems in order to understand the optical properties.

2. Experimental

Sub-stoichiometric $SiO_{1.5}$ thin films were deposited on top of Si (100) substrates by co-evaporation of SiO powder from a thermal cell and SiO_2 from an e-beam gun in an ultra-high vacuum chamber. The films thickness was 200 nm. The Ce doping was performed from a Knudsen cell heated at around 1400 °C. The Ce concentration was varied from 0.7 to 3 at.%. The samples were post-grown annealed in a rapid thermal annealing furnace under flowing N_2 at 1100 °C [22].

The 3D atomic scale characterization of the samples was carried out with a Laser-Assisted Wide-Angle tomographic Atom Probe (LAWATAP-Cameca) instrument. APT provides a 3D mapping of atoms contained in the sample. Further information on atom probe tomography and on the analysis conditions can be found elsewhere [25]. In an APT experiment, the specimens must be needle-shaped having an end-radius below 50 nm. The preparation of such tips was achieved by employing the lift-out and annular milling method [26,27], using a dual beam Zeiss NVision 40 FIB-SEM.

Photoluminescence (PL) measurements have been performed at room temperature using a 325 nm laser wavelength excitation. More information on the PL setup can be found in reference [24].

3. Results and discussion

3.1. Photoluminescence as a function of Ce content

Fig. 1 shows the PL spectra of Ce-doped $SiO_{1.5}$ thin films annealed at 1100 °C and measured at room temperature for various Ce concentrations. A broad emission band peaking in the range 350–650 nm is observed for all the samples. The emission at these wavelengths is commonly ascribed to the allowed electric dipolar 5d–4f transition of Ce^{3+} ions. For Ce contents up to 2 at.%, we can distinguish the presence of another luminescence band around 750 nm. The latter is due to radiative recombination between electrons and holes confined in the Si-nanoparticles formed in the films. Moreover, it is noteworthy that as the Ce content decreases, the Si-nanoparticles related PL intensity increases while simultaneously the Ce^{3+} related PL decreases. This behavior can possibly be due to an energy transfer between Si-nanoparticles and Ce^{3+} ions. Nevertheless, in their study, Weimmerskirch-Aubatin et al. [28] have shown by using photoluminescence excitation measurements on Ce-doped $SiO_{1.5}$ thin films that no energy transfer occurs in such system. We can thus rule out this hypothesis. Therefore, to understand the evolution of the optical properties, we investigated the nanostructural properties of the films by APT.

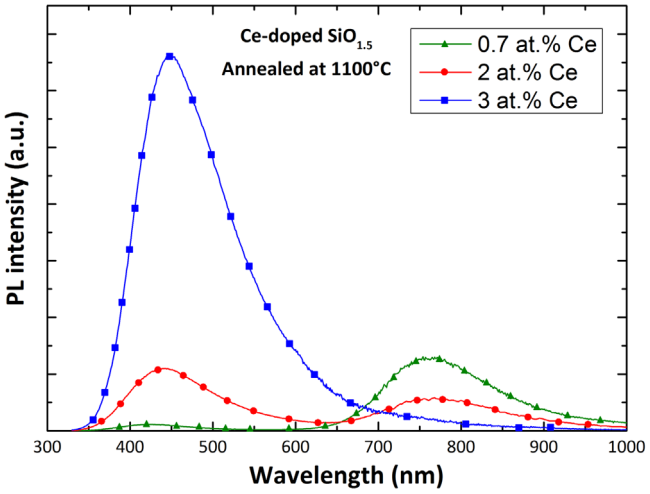

Fig. 1. Room temperature photoluminescence spectra of Ce-doped $SiO_{1.5}$ thin films annealed at 1100 °C as a function of Ce content varying between 0.7 at.% and 3 at.%.

3.2. Nanostructure analysis by atom probe tomography

The 3D reconstructions obtained from atom probe analysis on Ce-doped $SiO_{1.5}$ samples annealed at 1100 °C are presented in Fig. 2. 3D maps of pure Si-nanoparticles (red) and Ce-rich clusters (blue) are presented. For the sake of clarity, only Si atoms in Si-nanoparticles and Ce atoms from Ce-rich clusters, which also contain Si and O as explain later, are shown. The 0.7 at.% Ce-doped $SiO_{1.5}$ layer (Fig. 2a) contains a high density of Si-nanoparticles induced, as expected, by the phase separation of silicon in excess and the silica matrix. Moreover, the 3D reconstruction reveals also that some Ce-rich clusters exist. We can note that these Ce-rich particles are located in the vicinity of Si-ncs. Increasing the Ce-content up to 2 at.% leads to the formation high density of linked nanoparticles while some isolated Si-ncs are still observed (see dashed circles in Fig. 2b). Finally, for the film containing 3 at.% Ce, all Si-nanoparticles are remarkably located in the immediate vicinity of Ce-rich clusters. Thus, the 3D reconstructions obviously reveal that increasing the Ce content from 0.7 to 3% has a strong influence on the diffusion and growth of Si-nps.

In order to obtain a better insight of the nanostructural evolution of the samples, composition measurements are required. To determine the composition of the Ce-rich clusters quantitatively, a small box ($\sim 1x1 \times 1\ nm^3$) is placed in the core of each cluster. By counting the number of atoms of each species in the sampling box, we are able to identify the composition of the Ce-rich nanoparticle. The resulting compositional measurements of the Ce-Si-O nanoparticles are listed in Table 1. For the $SiO_{1.5}$ layer containing 0.7 at.% of Ce, the compositional analysis reveals that the Ce-rich clusters do not deal with any stable phase of Ce oxide, silicide or silicate. Similar results apply for the 2 at.% Ce-doped $SiO_{1.5}$ thin film despite the increase of the Ce content and the decrease of the Si concentration. Finally, for the sample containing 3 at.% Ce, the

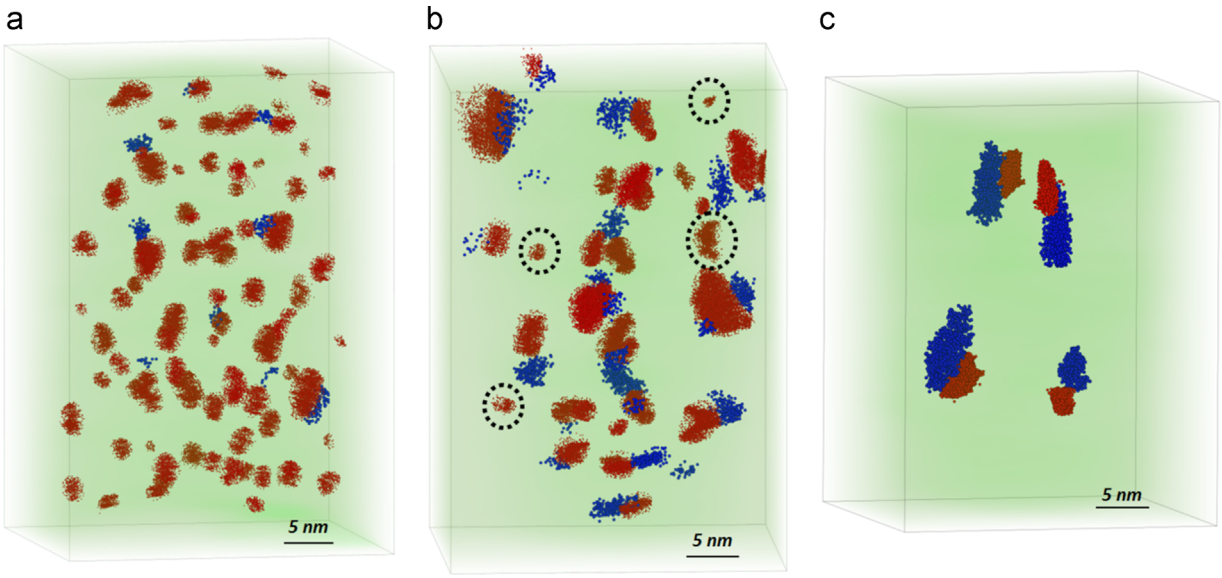

Fig. 2. 3D reconstructions of APT analysis of Si-ncs (red) and Ce-rich clusters (blue) for the a) 0.7 at.% b) 2 at.% and c) 3 at.% Ce-doped $SiO_{1.5}$ layers annealed at 1100 °C. (For interpretation of the references to color in this figure legend, the reader is referred to the web version of this article).

Table 1
Compositional measurements of Ce–Si–O nanoparticles (atomic percentages of Si, O and Ce).

Sample	Atomic concentration (at. %)			Stable phase
	Si	O	Ce	
0.7 at.% Ce	31.6 ± 0.6	58.0 ± 0.6	10.4 ± 0.4	
2 at.% Ce	23.4 ± 0.5	59.8 ± 0.5	16.8 ± 0.5	
3 at.% Ce	18.2 ± 0.4	65.5 ± 0.4	16.3 ± 0.4	$Ce_2Si_2O_7$

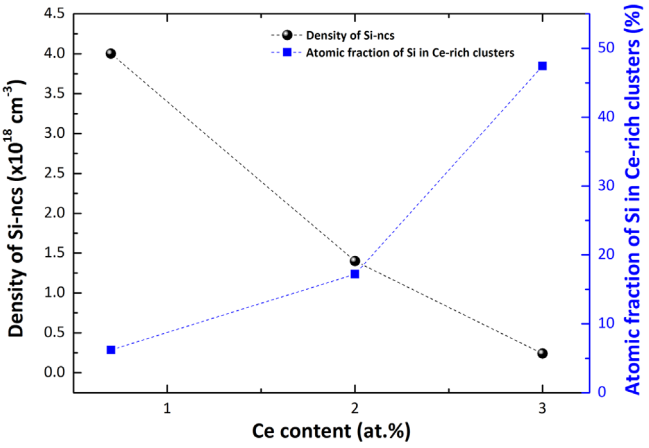

Fig. 3. Density of Si-ncs (left y-axis) and Si atomic fraction in Ce-rich clusters (right y-axis) as a function of Ce-content.

composition measurement is compatible with the formation of a cerium disilicate compound of stoichiometry $Ce_2Si_2O_7$. The matrix deals with a pure SiO_2 phase containing isolated Ce atoms ($\sim 7.10^{20} \pm 3.10^{20}$ at.cm^{-3}) which are not belonging to the Ce-rich clusters (not presented on Fig. 2). This result evidences that all the silicon atoms in excess, introduced during the elaboration, have segregated either in pure Si-ncs or in the Ce-rich clusters.

The evolution of the density of Si-ncs and of the atomic fraction of Si atoms in Ce-rich clusters as a function of Ce content are presented in Fig. 3. The number density of Si-ncs decreases as the Ce content increases and simultaneously the atomic fraction of Si atoms in Ce-rich clusters increases. This evolution is directly related to the influence of the Ce content on the growth of Si-ncs. Increasing the Ce content up to 3 at.% leads to the growth of Ce-rich clusters until the formation of $Ce_2Si_2O_7$. The atomic fraction of Ce atoms belonging to Ce-rich particles increases with the dopant concentration. Therefore, by increasing the Ce content, the formation of Ce disilicate nanoparticles requires more Si atoms. Thus, Si atoms in excess will remain in the $Ce_2Si_2O_7$ clusters rather than forming pure Si-ncs. Moreover, we have previously demonstrated that Si-ncs in 3 at.% Ce-doped layers are formed by two non-classical mechanisms [22]. Firstly, as observed in the case of the 0.7% Ce-doped $SiO_{1.5}$ layer, Si and possibly Ce atoms diffuse to form a Ce–Si–O rich phase. Secondly, Si atoms in this Ce-rich phase are ejected leading therefore to the growth of pure Si-ncs in the vicinity of Ce-silicate clusters. Increasing the Ce content up to 3 at.% leads to a control of Si-nps growth by Ce-silicate formation and therefore to no more isolated Si-ncs. For low dopant content, the amount of Ce atoms is not sufficient to form the $Ce_2Si_2O_7$ phase. In this case, isolated Si-ncs are formed as the initial silicon excess is constant for all the samples. The 2 at.% Ce-doped sample represents an intermediate case.

The observed nanostructures and the evolution of the phases in the films discussed above help us to understand the modification of the optical properties shown in Fig. 1. Indeed, the drop of the Ce^{3+} related PL intensities for the 0.7 and 2 at.% Ce-doped $SiO_{1.5}$ thin films may be related to the presence of a non-stable Ce-rich phase and the lack of formation of $Ce_2Si_2O_7$. As mentioned previously, a low amount of Ce^{3+} ions remains diluted in the SiO_2 matrix and can participate to the weak luminescence observed. Moreover, we can not exclude the formation of a small amount of $Ce_2Si_2O_7$ particles in the 2 at.% doped sample responsible of the increase in the PL between 0.7 at.% to 2 at.% doping. On the other hand, the intensity of the Si-ncs related PL decreases as the Ce content increases in the films. This feature is related to the increase of Si-ncs located in the vicinity of Ce-rich clusters when

the Ce content rises. Thus, the absence of Si-ncs related luminescence for the 3 at.% Ce-doped $SiO_{1.5}$ film is caused by the immediate proximity of the $Ce_2Si_2O_7$ nanoparticles which probably provide non-radiative recombination pathways. Finally, the Si-ncs PL detected in the sample containing 0.7 at.% and 2 at.% is attributed to the isolated Si-ncs observed in the layers (Fig. 2a and b.). The PL intensity decreases monotonously with the fraction of isolated Si-ncs.

4. Conclusions

In order to gain a better understanding of the optical properties of rare earth doped SiO_x thin films, a detailed investigation of the structure at the nanoscale is required. In this work, we have investigated, using atom probe tomography, the spatial localization of Si atoms and Ce ions in Ce-doped $SiO_{1.5}$ thin films. Our work allows to correlate the nanostructural evolution and the optical properties of Ce-doped $SiO_{1.5}$ thin films. The complex evolution of the Ce and Si related luminescence with Ce-content was explained. In particular, the strong PL emission from the layer containing 3 at.% Ce is related to the formation of a $Ce_2Si_2O_7$ compound. Moreover, for the 3 at.% Ce-doped layer, the quenching of the Si-nps related luminescence was explained by the location of all Si-nps in the immediate vicinity of $Ce_2Si_2O_7$ clusters. This was confirmed by the appearance of Si-nps related luminescence when isolated Si-nps were observed for lower Ce-contents. This demonstrates the effect of Ce on the precipitation mechanism in Ce-doped $SiO_{1.5}$ systems. This work brings a comprehensive view of the optical properties of Ce-doped SiO_x thin films in relation to their nanostructure. The correlation between these two aspects seems to be interesting and further work is required to fully master the formation of Ce-silicates nanoparticles and their luminescence. The control of the precipitation mechanism in such systems as a function of the elaboration conditions will open a new way to optimize the PL emission.

Acknowledgments

The authors would like to acknowledge the financial support of G. Beainy from the “Région Haute-Normandie”.

References

[1] L.T. Canham, Appl. Phys. Lett. 57 (10) (1990) 1046.
[2] T. Shimizu-Iwayama, S. Nakao, K. Saitoh, N. Itoh, J. Phys. Condens. Matter 6 (39) (1994) L601.
[3] A.J. Kenyon, P.F. Trwoga, C.W. Pitt, G. Rehm, J. Appl. Phys. 79 (12) (1996) 9291.
[4] K.D. Hirschman, L. Tsybeskov, S.P. Duttagupta, P.M. Fauchet, Nature 384 (6607) (1996) 338.
[5] B. Garrido Fernandez, M. López, C. García, A. Pérez-Rodríguez, J.R. Morante, C. Bonafos, M. Carrada, A. Claverie, J. Appl. Phys. 91 (2) (2002) 798.
[6] L. Pavesi, L. Dal Negro, C. Mazzoleni, G. Franzò, F. Priolo, Nature 408 (6811) (2000) 440.
[7] F.L. Bregolin, U.S. Sias, M. Behar, J. Lumin. 135 (2013) 232.
[8] Y.Q. Li, N. Hirosaki, R.-J. Xie, T. Takeda, M. Mitomo, J. Lumin. 130 (7) (2010) 1147.
[9] J.M. Sun, S. Prucnal, W. Skorupa, T. Dekorsy, A. Müchlich, M. Helm, L. Rebohle, T. Gebel, J. Appl. Phys. 99 (10) (2006) 103102.
[10] J.M. Sun, S. Prucnal, W. Skorupa, M. Helm, L. Rebohle, T. Gebel, Appl. Phys. Lett. 89 (9) (2006) 91908.
[11] J.M. Sun, W. Skorupa, T. Dekorsy, M. Helm, L. Rebohle, T. Gebel, J. Appl. Phys. 97 (12) (2005) 123513.
[12] L. Rebohle, J. Lehmann, S. Prucnal, A. Kanjilal, A. Nazarov, I. Tyagulskii, W. Skorupa, M. Helm, Appl. Phys. Lett. 93 (7) (2008) 71908.
[13] A. Nazarov, J.M. Sun, W. Skorupa, R.A. Yankov, I.N. Osiyuk, I.P. Tjagulskii, V.S. Lysenko, T. Gebel, Appl. Phys. Lett. 86 (15) (2005) 151914.
[14] R.L. Savio, M. Miritello, F. Iacona, A.M. Piro, M.G. Grimaldi, F. Priolo, J. Phys. Condens. Matter 20 (45) (2008) 454218.
[15] X.X. Wang, J.G. Zhang, B.W. Cheng, J.Z. Yu, Q.M. Wang, J. Cryst. Growth 289 (1) (2006) 178.
[16] J. Zheng, Y. Tao, W. Wang, L. Zhang, Y. Zuo, C. Xue, B. Cheng, Q. Wang, Mater. Lett. 65 (5) (2011) 860.
[17] J. Li, O. Zalloum, T. Roschuk, C. Heng, J. Wojcik, P. Mascher, Appl. Phys. Lett. 94 (1) (2009) 11112.
[18] A.H. Morshed, M.E. Moussa, S.M. Bedair, R. Leonard, S.X. Liu, N. El-Masry, Appl. Phys. Lett. 70 (13) (1997) 1647.
[19] W.C. Choi, H.N. Lee, E.K. Kim, Y. Kim, C.-Y. Park, H.S. Kim, J.Y. Lee, Appl. Phys. Lett. 75 (16) (1999) 2389.
[20] L. Kępiński, D. Hreniak, W. Stręk, J. Alloy. Compd. 341 (1) (2002) 203.
[21] J. Weimmerskirch-Aubatin, M. Stoffel, A. Bouché, P. Boulet, M. Vergnat, H. Rinnert, J. Alloy. Compd. 622 (2015) 358.
[22] G. Beainy, J. Weimmerskirch-Aubatin, M. Stoffel, M. Vergnat, H. Rinnert, C. Castro, P. Pareige, E. Talbot, J. Appl. Phys. 118 (2015) 234308.
[23] G. Beainy, J. Weimmerskirch-Aubatin, M. Stoffel, M. Vergnat, H. Rinnert, A. Etienne, P. Pareige, E. Talbot, Phys. Status Solidi C 12 (2015) 1313.
[24] J. Weimmerskirch-Aubatin, M. Stoffel, X. Devaux, A. Bouché, G. Beainy, E. Talbot, P. Pareige, Y. Fagot-Révurat, M. Vergnat, H. Rinnert, J. Mater. Chem. C 3 (2015) 12499.
[25] B. Gault, M.P. Moody, J.M. Cairney, S.P. Ringer, Atom Probe Microscopy, 160, Springer New York, New York, NY, 2012.
[26] K. Thompson, D. Lawrence, D.J. Larson, J.D. Olson, T.F. Kelly, B. Gorman, Ultramicroscopy 107 (2–3) (2007) 131.
[27] D.J. Larson, D.T. Foord, A.K. Petford-Long, H. Liew, M.G. Blamire, A. Cerezo, G.D. W. Smith, Ultramicroscopy 79 (1–4) (1999) 287.
[28] J. Weimmerskirch-Aubatin, M. Stoffel, X. Devaux, A. Bouché, M. Vergnat, H. Rinnert, Phys. Status Solidi C 11 (2014) 1630.